Controller Development for Reactive Power Flow Management Between DSO and TSO Networks

Katja Sirviö, Mike Mekkanen, Kimmo Kauhaniemi, Hannu Laaksonen
School of Technology and Innovations
University of Vaasa
Vaasa, Finland
forename.surname@uva.fi

Ari Salo
Vaasan Sähköverkko
Vaasa, Finland
ari.salo@vaasansahkoverkko.fi

Felipe Castro, Shoaib Ansari, Davood Babazadeh
Energy Division
OFFIS
Oldenburg, Germany
forename.surname @offis.de

***Abstract*—In the future, new solutions for active and reactive power control related to the flexibility services offered by distributed energy resources (DER) will be needed even more. One ancillary service which DER could provide is the reactive power flow management between DSO and TSO networks. This research aims to develop a reactive power controller from a preliminary algorithm to a light-weight IED for a wind turbine converter. The purpose of the controller is to maintain the reactive power flow of a medium voltage network within the limit set by a transmission system operator. In his paper, the controller development stages are presented - starting from the preliminary algorithm development by Simscape Power Systems to real hardware and testing it by Controller-Hardware-In-the-Loop simulations. The operation of the controller is investigated in the different development stages of the power network. The outcome is the development suggestions of the real-time simulation platform, as well as the discussion of further improvement possibilities for the controller.**

Keywords—Control Systems, Microgrids, Power system simulation, Testing

I. INTRODUCTION

Due to extensive integration of renewable generation at all voltage levels (HV, MV, and LV) new solutions to provide the needed technical ancillary, i.e., flexibility services are required in the future at local (DSO) and system-wide (TSO) levels. Among others, one specific flexibility service which distribution grid connected DER could provide is the reactive power (Q) flow management between different voltage levels and between DSO/TSO networks. However, to avoid unwanted interactions between the needs of different stakeholders, transparent coordination, and cooperation between TSOs and DSOs become increasingly important. [1] [2] [3]

So far, different control and management functions of microgrids have been studied, simulated, and tested [4], [5]. Pilot cases for different types of microgrids have emerged with early-stage microgrid controllers with vendor-defined characteristics [6].

The impact of standardization of product development can be illustrated as a general cycle of product sales and standardization [7]. The status of IEEE and IEC standards for microgrids, and especially for the control and management of microgrids, is still mostly in the development phase [8] [9] [10] [11] [12] [13] [14] [15] [16] [17]. However, real-life microgrid management solutions and their implementations are increasing rapidly globally. Some standards for microgrids have been published, but the standardization of microgrid controllers is still under development. Based on the state of the standardization, and available products, it can be concluded that microgrid controllers are in the stage "need to resolve issues related to product standards" [7]. The current issues of microgrid controllers relate to interoperability of different systems and functions that might comprise of solutions from different vendors, which comprises a microgrid. [18] [19]

These standards above establish the requirements for the microgrid controller at the point of interconnection (POI) [8]. One requirement for microgrid controllers is to offer ancillary services (AS). One possibility can be seen due to the requirements of reactive power flow at the HV/MV connection point set by the TSO for the DSO [20]. These kinds of issues should be considered when developing and testing the operation of microgrids and the microgrid controller functions.

Due to these issues, this research aims at developing a microgrid controller function in grid-tied mode, the technical AS for reactive power (Q) control. The control techniques for reactive power compensation in microgrids are generally implemented by converters for power quality and power control by droop strategies. In grid-tied mode, the microgrids can be used for reactive power control, thus transforming its operation into static VAR compensation [21], [22]. Authors did not find any similar reactive power control algorithm for DER that presented the preliminary controller [1] and wanted to develop the controller further. The algorithm is developed according to the "Reactive Power Window" (RPW) set by Fingrid, the Finnish TSO [20] or EPV Alueverkko who owns the sub-transmission HV network. A precursor algorithm of reactive power management for future Sundom Smart Grid (SSG) has been developed by offline simulations in [1] and [23], but in this research, the algorithm is developed further to fulfill the real-time requirements. The control algorithm for technical AS, managing reactive power flow at TSO/DSO interface is developed during the first stage with traditional offline simulations and after that tested as software-in-the-loop (SIL), as well as controller-hardware-in-the-loop (CHIL) in the real-time simulation and test platform.

In Section II, the network development scenarios of Sundom Smart Grid as well as the preliminary reactive power control algorithm with the traditional offline simulations by Simscape Power Systems are presented. Section III presents the development of RPW controller operation within the SIL and CHIL simulations on the real-time simulation platform. The conclusions and discussions are presented in Section IV.

II. REACTIVE POWER CONTROL AND NETWORK DEVELOPMENT SCENARIOS OF SUNDOM SMART GRID

Sundom Smart Grid (SSG) is a unique living lab pilot that is established in an MV network. The primary substation and

978-1-5386-8218-0/19/$31.00 ©2019 IEEE

four secondary substations are equipped with modern IEDs with fiber optic connections to each IED. A cloud service is set up to collect the IEC 61850 sampled values (SV) and GOOSE measurements from the network at 20 points. The measured SV data stream carries current and voltage measurements. The sampling rate is 80 samples per cycle or 4000 samples/s. Also, power, frequency, RMS voltages and currents, and other measurements are received by GOOSE messages. The University of Vaasa's Smart Grid laboratory and the SSG are connected with a direct communication link and the data collection facilities are used in various research activities. The GOOSE measurement data from the SSG is utilized for this research.

Three different basic structures of the network are developed with Simscape, with topologies expected for the years 2018, 2028 and 2035. These network scenarios differ on the expected demand growth, the increase of photovoltaic (PV) units, and cabling changes throughout the distribution system. These issues are presented in numbers in Fig. 1, where the line lengths and types are presented by the feeders: J06 Sulva, J07 Sundom, J08 Wind, and J09 Vaskiluoto. Also, the loads and PV generation are presented by the feeders. The total column presents overhead lines and cabling lengths as well as power demand and generation in the years 2018, 2028 and 2035. The cabling changes in the distribution system provide reactive power given that the demand expected by 2028 and 2035 is below the natural loading of the feeders.

These basic scenarios are simulated by SPS in phasor mode at 50 Hz. Fig. 2 presents the network structure of the simulation model. The main grid is modeled as a three-phase voltage source with the phase-to-phase voltage of 134.585 kV (the highest voltage based on primary transformer tap positions). The U_n of the primary transformer is 117/21 kV, and S_n is 16 MVA. In the following paragraphs, the developed use cases are presented, which are also presented in Table 1.

A. Situation 2018 and Scenario 2018s1

Situation 2018 is the base case presenting the current state. This use case aims at validating the simulation results and showing consistency with the real whole year measurements from the SSG. Hourly average values of active power generated from the measured GOOSE data over one year (1.5.2017 – 31.4.2018) are utilized in the model. The load profiles of the feeders J06 Sulva, J07 Sundom, and J09 Vaskiluoto are obtained from these measurements. In the same way, hourly average values of the measured active power generation of the 3.6 MW wind turbine (WT) are used as the generation data. Active power generation of the 33.6 kWp PV system at the Sundom school, connected to 0.4 kV, is modeled based on the estimation of solar irradiation data.

Based on the simulation results, the active power (P) flows of the simulation model are consistent with the measured data. The loads are modeled with a constant power factor to simplify the simulation. These power factors are estimated by calculating one-year power flows with different values of power factors. The best results are achieved by cosφ = 0.995 for all loads. The measured hourly reactive power according to active power (Q, P) values are presented in Fig. 3 and the simulated values in Fig. 4. It can be seen that the simulation results are in line with the measurements. Even though the results are slightly different because the OLTC was not modeled, the load types were not dynamic type, and the topology of the network is the same during the whole year

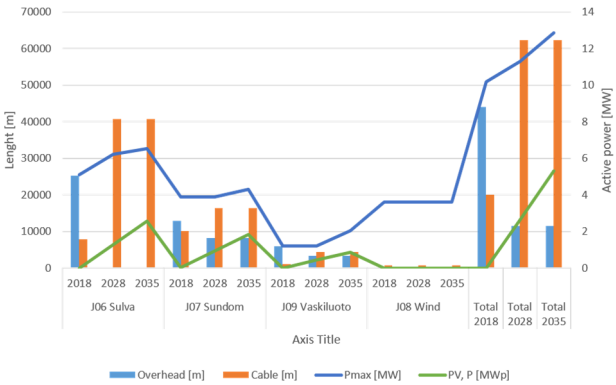

Fig. 1. The development of cabling, loads and generation in SSG.

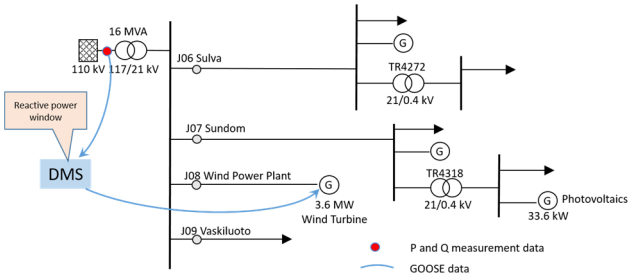

Fig. 2. Outline of the simulation model.

TABLE 1
The Simulation Scenarios

Scenario	Base network scenario	RPW control of WT	Shunt reactor 1.75 MVA
Status 2018	x		
Scenario 2018s1		x	
Scenario 2028s1	x		
Scenario 2028s2			x
Scenario 2028s3		x	x
Scenario 2035	x		

simulation (which was different to reality). This is acceptable and actually better for the evaluation of the RPW controller actions at the TSO's limits. The results are more accurate compared to the previous studies [1] [23], where the whole year load flow has been estimated based on one month's measurement data.

B. Scenario 2018s2

In this scenario, the RPW control is implemented through the WT converter and presented in the simulation model outline (Fig. 2). The measurements of active and reactive power are fed into the RPW controller, and the controller gives the reactive power set point (Q_{set}) as output for the WT converter. Fig. 5 presents the result of the simulation when the Q_{set} is set to the opposite of the measured reactive power at HV connection point (Q_{HV}) value if the reactive power according to active power (Q, P) point, is out of the window, i.e., $Q_{set} = \pm Q_{HV}$. In other words, the RPW algorithm always requires the reactive power to be set to zero at the POI if the (Q, P) point is out of the window. It can be noticed from Fig. 5 that all the points out of the window are controlled to "zero", except in the situation where reactive power is highly inductive. This is due to the variation of the voltage. The flowchart of the RPW algorithm part is presented in Fig. 6.

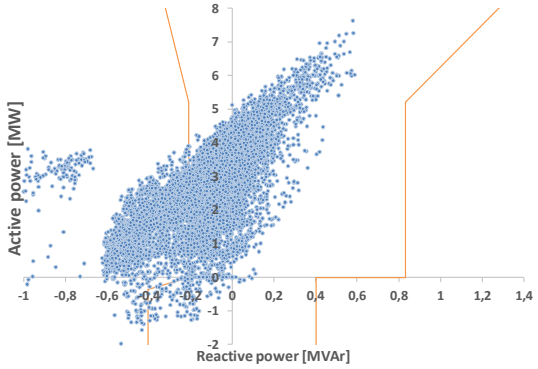

Fig. 3. Measured hourly active power as a function of measured reactive power in the TSO's reactive power window for the SSG.

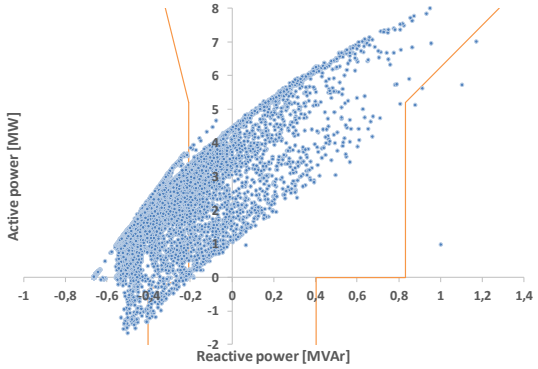

Fig. 4. Offline simulation, Simscape results of the Status 2018.

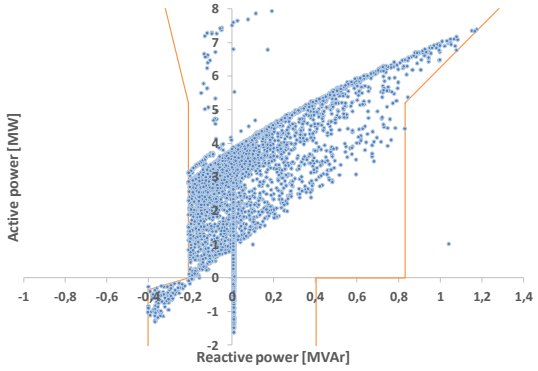

Fig. 5. Offline simulation, Simscape results of the Scenario 2018s2.

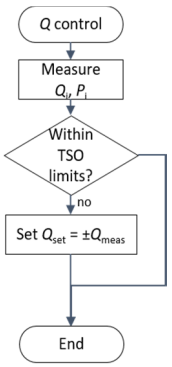

Fig. 6. Flowchart of the RPW control algorithm.

C. *Scenario 2028s1 and Scenario 2035s1*

In Scenario 2028s1, the grid is developed with increased cabling, loading, as well as the PV generation as presented in Fig. 1. The total cabling degree in the SSG will be increased from 20 km (31 %) up to 62 km (84 %) by the year 2028. The peak load is estimated to increase from 10 MW up to 11 MW. The PV generation increase is estimated to be up to 2.6 MWp in total at feeders J06, J07, and J09. In this scenario, the reactive power is all the time capacitive, and the TSO's limits are mostly exceeded.

In Scenario 2035s1, the grid is developed further with loading as well as the increase of the PV generation that is also presented in Fig. 1. The cabling situation is the same than in the year 2028. The peak load is estimated to increase up to 12.8 MW, and the PV generation is estimated to be up to 5.3 MWp in total. Compared to the Scenario 2028, the (Q, P) situation is quite the same.

III. Development of the RPW Controller Operation

Several types of scenarios are developed with Simscape, as presented in Table 1. The scenarios differ based on the control; in scenarios 2028, there is also a shunt reactor (SR) implemented to the MV bus. The same network scenarios are modeled with ePHASORSIM, and the SIL offline results are compared to the SPS simulations with the one-year load flow of the basic network without RPW control. After that, the RPW controller is modified for operating as closed-loop control during long-term simulations. In other words, the RPW controller is adapted for the real-time digital simulation platform and is improved.

A. *Scenario 2018s2*

The offline simulations by the real-time model(s) are performed for the SSG where the reactive power is controlled by the RPW controller as closed-loop. The controller includes the algorithm almost like the same as in the SPS model, but also, an I-controller is utilized to achieve stability of the controlled power system. Also, a hold/memory block is inserted to maintain the Q_{set} as long as the measured reactive and active power points (Q_{meas}, P_{meas}) stay inside the RPW.

The RPW control algorithm is also modified differing from the open loop model. Instead of controlling Q_{HV} to zero if the (Q_{meas}, P_{meas}) point is out of the window (as in Simscape model) the output of the algorithm Q_{set} is such that reactive power at the POI would be set to the RPW limits. This modification is necessary because when $Q_{set} = \pm Q_{HV}$ the reactive power at the WT converter is oscillating as well as at the 110 kV connection point.

Next, it is noticed that by controlling the reactive power exactly to the RPW limits at the POI gives the result that not all the points are inside the window. This happens because the controller is adaptive and measurements from HV connection points are lagging/delayed compared the output (Q_{set}) of the controller with one input data reading cycle T_d and one simulation step. In other words, the average hourly reactive power according to the average hourly active power (Q_{HVavg}, P_{HVavg}) points at the POI are calculated as hourly average values in which T_d is affecting (and the calculation was based on the T_s). Consequently, there are more points for calculating the hourly moving averages when $T_d = 1$. Since the $T_s = 0.01$ s, there are 100 measurement points within a simulated hour. In the situation $T_d = 0.1$ there are 10 measurement points within a simulated hour. Therefore by setting the RPW limits ± 50 kVAr tighter, except $QD_1 = 200$ kVAr (the feed-in Q when consuming P) it is possible to imitate slightly and easily predictive control. Another option could be to develop an estimator, but this development work is left to the future. Now the active power of the WT is peaceful, and all the points are inside the window.

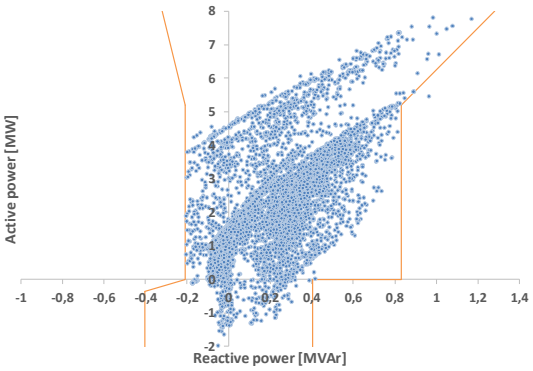

Fig. 7. SIL offline simulation of the Scenario 2018s2. RPW of the SSG when the input data is step function and $T_d = 0.1$.

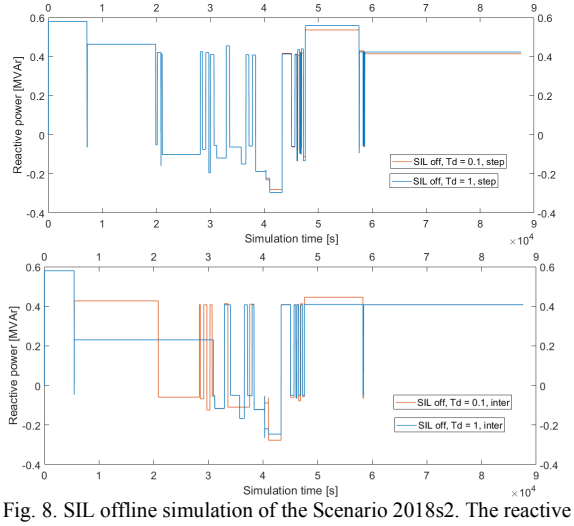

Fig. 8. SIL offline simulation of the Scenario 2018s2. The reactive power of the WT converter when the input data is either step function or interpolated as well as $T_d = 0.1$ or $T_d = 1$. The RPW controller is set up to the TSO limits ± 50 kVAr, except $QD_1 = 200$ kVAr.

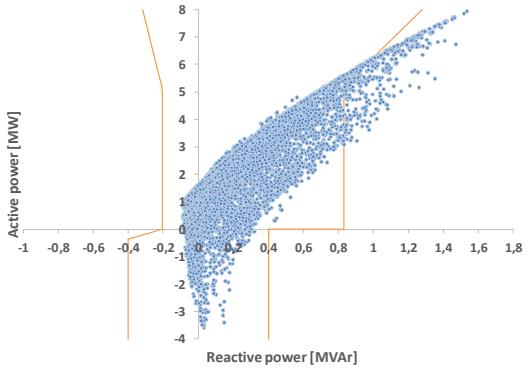

Fig. 9. Offline simulation of the Scenario 2028s2. RPW of the SSG when the input data was step function and $T_d = 0.1$.

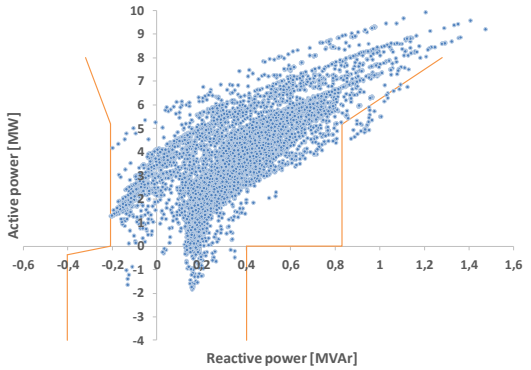

Fig. 10. SIL offline simulation of the Scenario 2028s4. RPW of the SSG when the input data is step function and $T_d = 0.1$. The RPW controller is set up to the TSO limits ± 50 kVAr, except $QD_1 = 200$

Furthermore, the RPW controller operation is tested with a different type of input data that either is a step function or interpolated. Fig. 8 presents simulation results, the reactive power window (with the tuned RPW controller), when the $T_d = 0.1$, and when the input data is a step function. The result is similar with interpolated data. The difference can be noticed against the results of the open loop simulations (Fig. 5). Fig. 8 presents, in turn, the reactive power of the WT converter when the RPW controller is set up to the TSO limits ± 50 kVAr, except $QD_1 = 200$ kVAr, and when the input data is either step function or interpolated as well as when $T_d = 0.1$ or $T_d = 1$. It can be noticed that there is a difference in the controlled reactive power depending on the input data; type and time step. The controller is calculating a new value for the Q_{set} in every simulation step (10 ms), so naturally, the Q_{set} differs between the simulations based on the step or interpolated data. Despite that, it can be noticed that the results are almost the same when the input data is step function or interpolated, but the number of the control actions for the converter is slightly less when the data is interpolated (that is closer to the real world measurement data). In the real world, $T_d = 1$ would represent measurement data coming from POI in every 36 s and $T_d = 0.1$ would represent every 360 s (6 min).

B. *Scenario 2028s3*

In this scenario, a 1.75 MVAr shunt reactor (SR) is applied for consuming the reactive power at the 20 kV bus. Fig. 9 presents the simulation results when the SR is applied. It can be noticed that almost all the points are inside the window. The RPW controller takes care of staying inside the RPW limits. This scenario is tested by the different variations of set-ups; the input data is either step function or interpolated, the SR is either constant Q or voltage-dependent, the limits for the RPW controller varies from TSO limits ±0, ±50 to ±100 kVAr. Fig. 10 presents results when the RPW limits are set according to the TSO limits ±50 kVAr, except $QD_1 = 200$ kVAr. By comparing the results the case TSO limits and the case TSO limits ± 50 kVAr, the latter gives slightly better results in the reactive power window (like in Scenario 2018s1), but much better results in the WT converter control point of view.

IV. Comparison of Tests

The SIL offline, SIL real-time, and CHIL tests are compared. The outline of the simulation platform is presented in Fig. 11. The presented use case is 2018s2, and the RPW controller set-up limits are TSO ± 50 kVAr, except $QD_1 = 200$ kVAr, and the data reading step T_d is 1. The hardware used is

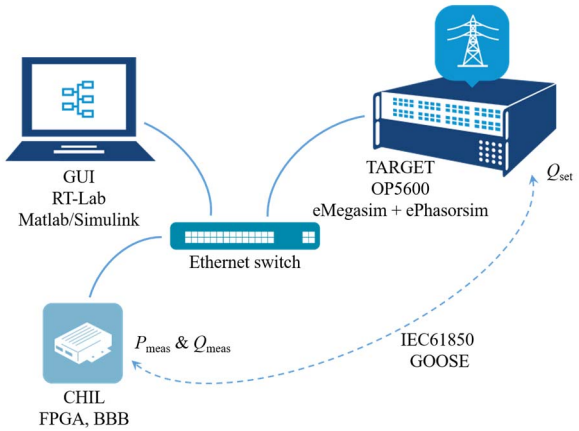

Fig. 11. The real-time simulation platform. [26]

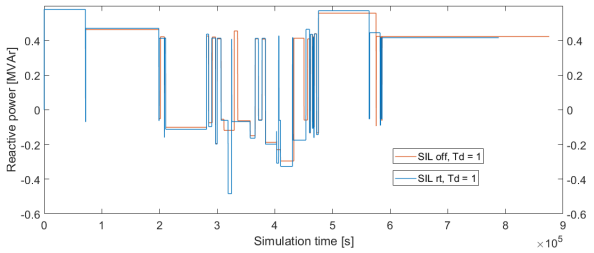

Fig. 12. SIL offline simulation of Scenario 2018s2. Reactive power of the WT converter when the input data is step function and Td = 1. The RPW controller is set up to the TSO limits ± 50 kVAr, except QD_1 = 200 kVAr.

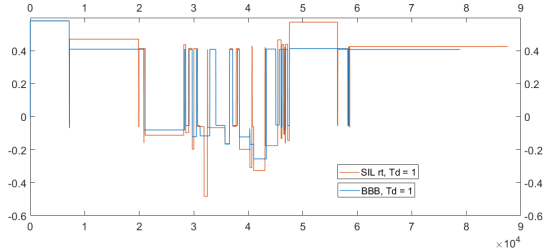

Fig. 13. SIL real-time simulation and CHIL test of Scenario 2018s2. Reactive power of the WT converter when the input data is step function and Td = 1. The RPW controller is set up to the TSO limits ± 50 kVAr, except QD_1 = 200 kVAr.

BeagleBoneBlack (BBB). Fig. 12 presents the results of SIL offline and SIL real-time simulations. There is a slight difference between the results that have to depend on communication delays that are affecting the control. Fig. 13 presents the comparison between SIL real-time and CHIL with BBB. It can be noticed that there is a difference caused by the processor/processing time of the used hardware.

V. Conclusion

In this research, the RPW controller was developed from a SIL controller to real hardware. The simulations bring into question that the RWP controller could be predictive to define the RPW limits simply according to the TSO's requirements. This development demonstrated that for long-term tests and simulation studies, a suitable coefficient for T_d could be defined to present, e.g., one-year study cases reliable enough. Also, the effect of the communication delay was demonstrated in real-time simulations and was compared to offline simulation results. Thus, in the CHIL tests, also the processing time of the hardware affected the results.

We propose that for the further development of an RPW controller a long-term real-time simulation platform or test set-up should be defined and developed in which a predictive RPW controller could be tested to take in account the communication delays and the processing time of the hardware in CHIL tests.

Acknowledgment

This simulation study has been performed using the ERIGrid Research Infrastructure and is part of a project that has received funding from the European Union's Horizon 2020 Research and Innovation Programme under the Grant Agreement No. 654113. The support of the European Research Infrastructure ERIGrid and its partner OFFIS e.V. is very much appreciated.

References

[1] K. Sirviö, H. Laaksonen and K. Kauhaniemi, "Active network management scheme for reactive power control," in *Cired Workshop*, Ljubljana, Slovenia, 2018.

[2] S. Uebermasser, C. Groiss, A. Einfalt, N. Thie, M. Vasconcelos, J. Helguero, H. Laaksonen and P. Hovila, "Requirements for coordinated ancillary services covering different voltage levels," *CIRED - Proceedings Journal,* vol. 1, pp. 1421-1424, 2017.

[3] H. Laaksonen, K. Sirviö, S. Aflecht, and P. Hovila, "Multi-objective Active Network Management Scheme Studied in Sundom Smart Grid with MV and LV Network Connected DER Units," in *CIRED Conference on Electricity Distribution*, Madrid, Spain, 2019.

[4] S. Sen and V. Kumar, "Microgrid control: A comprehensive survey," *Annual Reviews in Control,* vol. 45, pp. 118-151, 2018.

[5] F. M. Zia, E. Elbouchikhi and M. Benbouzid, "Microgrids energy management systems: A critical review on methods, solutions, and prospects," *Applied Energy,* vol. 222, pp. 1033-1055, 2018.

[6] G. Liu, M. R. Starke, and D. Herron, "Microgrid Controller and Advanced Distribution Management Survey Report," Oak Ridge National Laboratory (ORNL), Oak Ridge, US, 2016.

[7] J. Reilly, A. Hefner, B. Marchionini and G. Joos, "Microgrid Controller Standardization - Approach, Benefits and Implementation," in *CIGRE Grid of the Future Symposium*, Cleveland, US, 2017.

[8] "IEEE Standard for the Specification of Microgrid Controllers," *IEEE Std 2030.7-2017,* pp. 1-43, 2018.

[9] "IEEE Standard for the Testing of Microgrid Controllers," *IEEE 2030.8-2018,* pp. 1-42, 2018.

[10] IEEE, "P1547-2018 Interconnection and Interoperability of Distributed Energy Resources with Associated Electric Power Systems Interfaces," 2018.

[11] IEC, "Microgrids - Part 1: Guidelines for microgrid projects planning and specification," *Standard,* p. 33, 2017.

[12] IEC, "Microgrids - Guidelines for Operation (and Control)," 2018.

[13] IEEE, "IEEE 2030.9-2019 - IEEE Approved Draft Recommended Practice for the Planning and Design of the Microgrid," 2019.

[14] IEEE, "P2030.10 - Standard for DC Microgrids for Rural and Remote Electricity Access Applications," 2019.

[15] IEC, "IEC TS 62898-3-1 ED1, Microgrids - Part 3-1: Technical requirements - Protection and dynamic control," 2019.

[16] IEC, "IEC TS 62898-3-2 ED1, Microgrids – Part 3-2: Technical requirements - Energy management systems," 2019.

[17] IEC, "IEC TS 62898-3-3 ED1,Microgrids - Part 3-3: Technical requirements – Self-regulation of dispatchable loads," 2019.

[18] J. Ballieul, M. C. Caramanis, and M. Ilic´, "Control Challenges in Microgrids and the Role of Energy-Efficient Buildings," *Proceedings of the IEEE,* vol. 104, no. 4, pp. 692-696, 2016.

[19] J. Reilly and G. Joos, "Microgrid Controller Standards for Integration and Interoperability," in *CIRED Workshop*, Ljubljana, 2018.

[20] Fingrid, "Supply of Reactive Power and Maintenance of Reactive Power Reserves - Guideline," Fingrid, 2017.

[21] M. Gayatri, A. M. Parimi, and A. P. Kumar, "Reactive Power Compensation in Microgrids: A Survey Paper," *Renewable and Sustainable Energy Reviews,* vol. 81, no. 1, pp. 1030-1036, 2018.

[22] A. Á. Téllez, G. López, I. Isaac, and J. W. Gonzalez, "Optimal Reactive Power Compensation in Electrical Distribution Systems with Distributed Resources," *Heliyon,* vol. 4, no. 8, 2018.

[23] K. Sirviö, L. Välkkilä, H. Laaksonen, K. Kauhaniemi and A. Rajala, "Prospects and Costs for Reactive Power Control in Sundom Smart Grid," in *IEEE ISGT Europe*, Sarajevo, 2018.

[24] Fingrid, "Supply of reactive power and maintenance of reactive power reserves," Guideline.

[25] M. Gayatri, P. M. Alivelu, and A. P. Kumar, "A Review of Reactive power Compensation Techniques in Microgrids," *Renewable and Sustainable Compensation Techniques in Microgrids,* vol. 81, pp. 1030-1036, 2016.

[26] K. Sirviö, M. Mekkanen, K. Kauhaniemi, and D. Babazadeh, "Sundom Hardware-In-the Loop Living Lab - Technical Report," 2019.